INSTITUTE OF PHYSICS PUBLISHING JOURNAL OF OPTICS B: QUANTUM AND SEMICLASSICAL OPTICS

J. Opt. B: Quantum Semiclass. Opt. **6** (2004) S190–S196 PII: S1464-4266(04)71466-4

Counterpropagating self-trapped beams in photorefractive crystals

M Belić[1], Ph Jander[2], K Motzek[3], A Desyatnikov[2], D Jović[1], A Strinić[1], M Petrović[1], C Denz[2] and F Kaiser[3]

[1] Institute of Physics, PO Box 57, 11001 Belgrade, Serbia
[2] Institute of Applied Physics, Westfälische Wilhelms-Universität Münster, D-48149 Münster, Germany
[3] Institute of Applied Physics, Darmstadt University of Technology, Hochschulstraße 4a, D-64289 Darmstadt, Germany

Received 31 October 2003, accepted for publication 12 January 2004
Published 4 May 2004
Online at stacks.iop.org/JOptB/6/S190
DOI: 10.1088/1464-4266/6/5/005

Abstract
A time-dependent model for the formation of self-trapped optical beams in photorefractive media by counterpropagating laser beams is analysed. It is shown that dynamically the beams may form stable steady-state structures or display periodic and irregular temporal behaviour. Steady-state solutions of non-uniform cross section are found, representing a general class of self-trapped waveguides, that include counterpropagating spatial vector solitons as a particular case. Two critical curves are identified in the plane of parameters, the first one separating vector solitons from the stable bidirectional waveguides and the second one separating stable waveguides from the unstable ones. Dynamically stable rotating beam structures are discovered that have no analogues in the usual steady-state theory of spatial solitons.

Keywords: nonlinear optics, counterpropagating beams, transverse effects, photorefractive crystal

(Some figures in this article are in colour only in the electronic version)

1. Introduction

Thus far spatial screening solitons [1] have been considered almost exclusively in the copropagation geometry. A few exceptions exist, notably the investigations by Haelterman *et al* [2], in which bimodal counterpropagating (CP) solitons in Kerr media have been treated, and by Cohen *et al* [3], in which collisions of solitons propagating in opposite directions, in both Kerr and local photorefractive (PR) media, have been addressed. Both accounts have been in one transverse dimension (1D) and steady-state. However, it is known that CP wave mixing geometries in PR media are prone to instabilities [4–6]. In fact, such geometries are often employed for transverse optical pattern formation in 2D [7]. On the other hand, one may easily envisage interest in the stable self-adjustable bidirectional connection of two arrays of beams across a PR crystal. It is therefore of interest to investigate the behaviour of CP beams in PR crystals in 2D, under conditions favourable to the formation of self-trapped optical structures.

In this paper we review some of the known features of CP self-trapped beams in PR media and add new results. We analyse equations for the propagation and interaction of CP beams, similar to the equations for the bimodal CP solitons in Kerr media [2], or the colliding screening solitons in PR crystals [3]. We formulate a time-relaxation procedure for the determination of space charge field and refractive index modulation in PR crystals, which serve as an input to the propagation equations. We display numerically the temporal formation of bright spatial screening vector solitons formed by CP beams, and discuss their interactions in (1 + 1) and (2 + 1) spatial dimensions. Beyond soliton solutions, we introduce a more general class of steady-state induced waveguides, that arise through a symmetry breaking transition of solitons. Additionally, situations where the interacting beams do not converge to a stationary structure, but alternate between different states, are reported. Dynamical effects are found important for understanding the behaviour of CP beams.

Finally, stable rotating beam structures are presented that have no analogues in the copropagating geometry. Such dynamical states cannot be accessed by the usual steady-state [1] theories of spatial solitons.

Section 2 of the paper introduces the model. The refractive index change is connected to the space charge field, and introduced into the paraxial propagation equations. In section 3 results concerning the (1 + 1)D case are presented. Stable and time-dependent solutions in the form of simple bidirectional waveguides and dipole-mode vector solitons are depicted. The symmetry breaking transition of CP solitons into bidirectional waveguides is found, and a critical curve in the plane of parameters determined. A second critical curve in the parameter plane is identified, separating stable waveguides from the unstable ones. Differences between coherent and incoherent interaction of CP beams are highlighted, and a transverse symmetry-breaking dynamical solution with complicated beam structure is presented. Section 4 deals with the (2 + 1)D results in the form of dipole-mode vector solitons and rotating dipoles. An example of colliding vortices with opposite topological charges is shown, leading to a stable rotating state. Section 5 brings conclusions.

2. The model

2.1. Refractive index modulation

We consider CP light beams in a PR crystal, in the paraxial approximation, under conditions suitable to the formation of spatial screening solitons [8]. As a working example we adopt experimental data [9] on the Nd:YAG laser at 532 nm, illuminating an SBN:Ce60 crystal. The optical field is given as the sum of waves $F\exp(\mathrm{i}kz+\mathrm{i}\omega t)+B\exp(-\mathrm{i}kz+\mathrm{i}\omega t)$ counter-propagating along the z direction, k being the wavevector in the medium, and F and B are the slowly varying envelopes of the beams. The light intensity I is measured in units of the background light intensity, necessary for the generation of solitons. After averaging in time on the scale of response time τ_0 of the PR crystal, the total intensity is given by:

$$1 + I = (1 + I_0)\{1 + \varepsilon[m\exp(2\mathrm{i}kz) + \text{c.c.}]/2\}, \qquad (1)$$

where $I_0 = |F|^2 + |B|^2$, $m = 2FB^*/(1 + I_0)$ is the modulation depth and c.c. stands for complex conjugation. Here the parameter ε measures the degree of temporal coherence of the beams related to the crystal relaxation time. For $\varepsilon = 0$, i.e. when the relative phase of the beams varies much faster than τ_0, the beams are effectively incoherent. In the opposite case $\varepsilon = 1$, the intensity distribution contains an interference term which is periodically modulated in the direction of propagation z, chosen to be perpendicular to the c-axis of the crystal, which is also the x-axis of the coordinate system. Beams are polarized in the x direction, and the external electric field E_e, necessary for the formation of self-trapped beams, also points in the x direction.

The electric field in the crystal couples to the electro-optic tensor, giving rise to a change in the index of refraction of the form

$$\Delta n = -\frac{n_0^3}{2} r_\mathrm{eff} E_\mathrm{tot}, \qquad (2)$$

where n_0 is the unperturbed index, r_eff is the effective component of the electro-optic tensor (in this case r_{33}), and E_tot is the x-component of the total electric field. It consists of the external field E_e and the space charge field E_sc generated in the crystal, $E_\mathrm{tot} = E_\mathrm{e} + E_\mathrm{sc}$.

2.2. Space charge field

The light intensity modulates the space charge field, which is represented in the normalized form

$$E_\mathrm{sc}/E_\mathrm{e} = E_0 + \tfrac{1}{2}[E_1\exp(2\mathrm{i}kz) + \text{c.c.}] \qquad (3)$$

where E_0 is the homogeneous part of the x-component of the space charge field, and $E_1(x, z)$ is the additional slowly varying part of the space charge field proportional to ε, $|\partial_z E_1| \ll 2k|E_1|$. It is E_0 that screens the external field, and E_1 is the result of the interference pattern along the z direction. It vanishes together with the intensity modulation for incoherent beams, i.e. in the limit $\varepsilon = 0$.

In a simplified approach, one assumes a local, isotropic approximation to the space charge field, and looks for a solution with saturable nonlinearity $E_\mathrm{tot} = E_\mathrm{e}/(1 + I)$. Substituting equations (1) and (3) in this expression, neglecting higher harmonics and terms quadratic in m, we obtain as a steady-state solution

$$E_0 = -\frac{I_0}{1 + I_0}, \qquad E_1 = -\frac{\varepsilon m}{1 + I_0}. \qquad (4)$$

The temporal evolution of the space charge field is assumed to be a relaxation-type dynamics [10]

$$\tau\partial_t E_0 + E_0 = -\frac{I_0}{1 + I_0}, \qquad (5a)$$

$$\tau\partial_t E_1 + E_1 = -\frac{\varepsilon m}{1 + I_0}, \qquad (5b)$$

where the relaxation time of the crystal τ is inversely proportional to the total intensity $\tau = \tau_0/(1 + I)$, i.e. illuminated regions in the crystal react faster. The assumed dynamics is that the space charge field builds up towards the steady-state, which depends on the light distribution, which in turn is slaved to the slow change of the space charge field. As will be seen later, this type of dynamics does not preclude a more complicated dynamical behaviour.

2.3. Propagation equations

Selecting synchronous terms in the nonlinear paraxial wave equation, one obtains propagation equations of the form

$$\mathrm{i}\partial_z F + (\partial_x^2 + \partial_y^2)F = \Gamma[E_0 F + E_1 B/2], \qquad (6a)$$

$$-\mathrm{i}\partial_z B + (\partial_x^2 + \partial_y^2)B = \Gamma[E_0 B + E_1^* F/2], \qquad (6b)$$

where $\Gamma = (kn_0x_0)^2 r_\mathrm{eff} E_\mathrm{e}$ is the coupling strength, and the rescaling $(x, y) \to (x/x_0, y/x_0)$, $z \to z/L_\mathrm{D}$, $(F, B) \to (F, B)\exp(-\mathrm{i}\Gamma z)$ is used. Here x_0 is the typical beam waist and $L_\mathrm{D} = 2kx_0^2$ is the diffraction length. Propagation equations can be put in a universal dimensionless form that contains no parameters or coupling constants. All the parameters are then hidden in the scaling quantities and the initial and boundary conditions. We prefer the form given here, with one explicitly given intensive control parameter Γ.

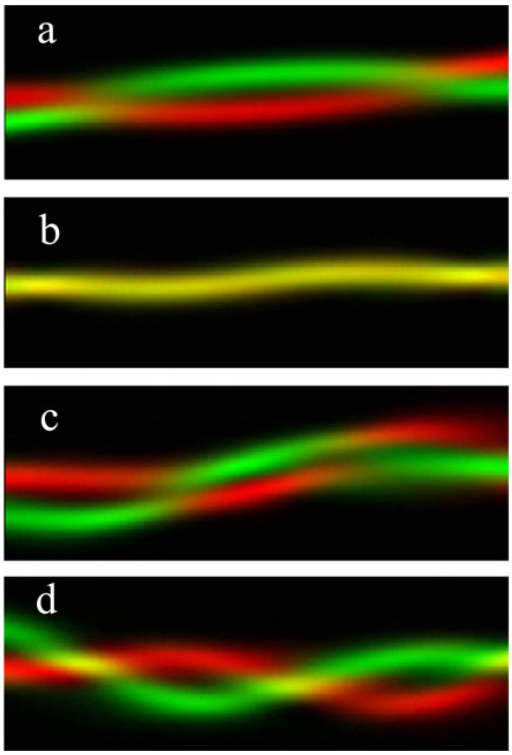

Figure 1. Bidirectional waveguide in the (x, z) plane. (a) Total intensity distribution in a stable configuration, for $\Gamma = 3$ and the propagation distance $L = 10L_{\mathrm{D}}$. (b)–(d) Unstable configuration for the same Γ and for $L = 15L_{\mathrm{D}}$. (b) Developing modulational instability at time $t = 20\tau_0$. (c) Unstable configuration at $t = 60\tau_0$. (d) Unstable configuration at $t = 90\tau_0$. Initial peak intensities are $I_F = I_B = 1.5$, $\varepsilon = 0$, transverse data size 10 beam waists.

The corresponding extensive control parameter is the crystal length L.

The propagation equations are solved numerically, concurrently with the temporal equations. The numerical procedure consists in solving equations (5) for the components of the space-charge field in time, with the light fields obtained at every step as guided modes of the induced common waveguide. This is achieved by an internal spatial relaxation loop, i.e. nested within the temporal loop, based on a beam-propagation method for the right- and left-propagating components. Both loops are iterated until convergence, which however is not necessarily reached in the temporal loop. In that case a time-dependent, dynamical state is obtained. The procedure is described in [6, 11].

3. One-dimensional results

3.1. Counterpropagating solitons and waveguides

We consider first the results in (1+1) spatial dimensions. Head-on collision of beams with appropriate initial conditions and parameter values, after temporal relaxation to a steady-state, results in the formation of a CP soliton, similar to the one found in [3]. Shooting initial beams with arbitrary parameters generally leads to a z-dependent non-stationary character of the beam propagation. In some domain of the initial parameters, for example with the relative angle of beam scattering θ close to π and small initial transverse offset, our time-relaxation procedure converges to stationary structures, which we denote as steady-state self-trapped waveguides.

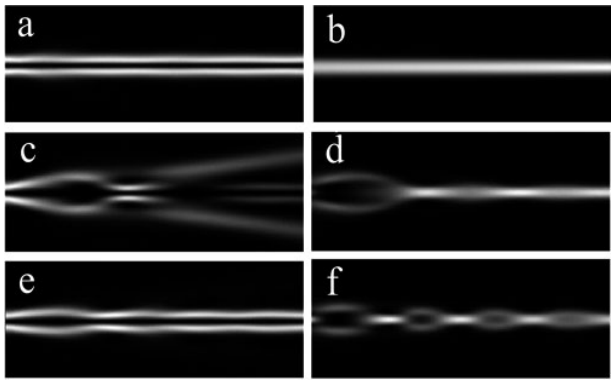

Figure 2. Counterpropagating dipole-mode vector soliton, (x, z) cross section. Left column, the dipole component, propagating to the right. Right column, the fundamental beam, propagating to the left. (a) and (b) Stable configuration for $\Gamma = 10/3$ and the beam intensities $I_F = I_B = 2$. (c) and (d) Unstable configuration for the same Γ, but for an increased intensity of the dipole beam, $I_F = 5$, at time $t = 50\tau_0$. (e) and (f) The same configuration as in (c) and (d), but at $t = 100\tau_0$. The propagation distance is 40 L_{D}, $\varepsilon = 0$. The transverse size of data windows is 20 beam diameters. The unstable configurations repeat themselves after approximately $130\tau_0$ steps.

The formation and dynamics of a single bidirectional waveguide is shown in figure 1. Two incoherent Gaussian beams are launched at different lateral positions perpendicular to the crystal edges, $\theta = \pi$. When the initial separation is 4 or more beam diameters, the beams hardly feel the presence of each other, and focus into individual solitons. For the separation of 1 beam diameter the interaction is strong enough for the beams to form a joint waveguiding structure. Both beams diffract initially, until the space charge field is developed in time to form the waveguide induced by the total light intensity, and this induced waveguide traps both beams (figure 1(a)). If, however, the propagation distance is increased from $10L_{\mathrm{D}}$ to $15L_{\mathrm{D}}$, a modulational instability develops, which prevents the beam configuration from converging (figures 1(b)–(d)). It changes continually, without repeating configurations in the limited time of observation. Such dynamical states are impossible to reach by the usual steady-state analyses of spatial solitons [1].

One can easily generalize this approach, by introducing higher-order CP solitons, similar to the multihump vector solitons in copropagating geometry (see, e.g. [12]). In figure 2 we present a particular case of a dipole-mode CP soliton. A dipole beam is launched from the left, and a power-matched single beam from the right. Such a bimodal CP soliton has been studied in [2] and has been found to be stable in the copropagating geometry [12]. A stable dipole-mode CP soliton is presented in figures 2(a) and (b). When the intensity of the dipole component is increased from 1.5 to 5, after an initial convergence to a dipole-mode soliton, a modulational instability develops, which forces a periodic repetition of the beam configuration after approximately $130\tau_0$ intervals. Typical phases are depicted in figures 2(c)–(f).

We would like to note here that not only for increasing propagation distances, i.e. for larger crystal thicknesses, and for increasing beam intensities, but also for increasing coupling

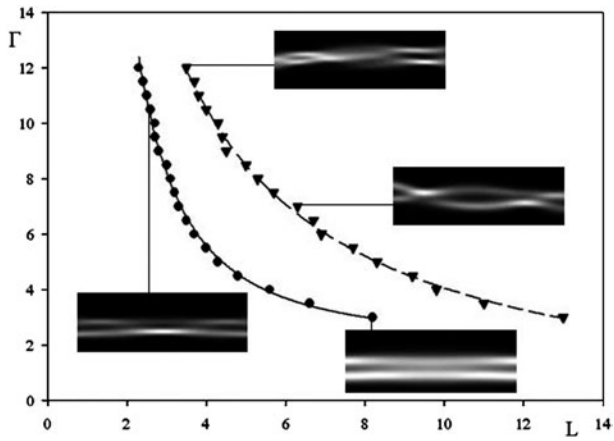

Figure 3. Critical curves in the parameter plane for the existence of stable CP solitons, bidirectional waveguides and unstable solutions (1D). L is given in units of L_{D}, and Γ is a dimensionless quantity. Below the first curve CP solitons exist, between the curves bidirectional waveguides appear. At and above the second curve unstable solutions emerge. Insets depict typical beam intensity distributions in the (x, z) plane at the points indicated. The points are numerically determined, the curves are inverse power polynomial fits.

strengths the development of longitudinal modulational instabilities in time is observed, even for the initial beams corresponding to the exact steady-state solitons. Modulational instability is a topic of ongoing research and beyond the framework of the present paper. Linear stability and nonlinear dynamical analyses will be reported elsewhere. Here we present threshold curves and a characteristic dynamical behaviour, obtained numerically.

3.2. Symmetry breaking transition

To capture the transition from a CP soliton to a waveguide more clearly, we consider the head-on collision of two identical Gaussian beams. In the absence of the other, each beam focuses into a soliton. We are interested in what happens when they are both present, and when the coupling constant Γ and the crystal length L are both varied. The situation is displayed in figure 3. It is seen that in the plane (L, Γ) of control parameters there exists a critical curve below which stable CP solitons exist (the first curve in figure 3). At that critical curve a new type of solution appears, in which the two components no longer overlap, but split and cross each other. A few examples are depicted in the insets in figure 3. As the beams split, a portion of each beam remains guided by the other, therefore we term these solutions bidirectional waveguides. Both the solitons and waveguides are steady-state solutions.

As one moves away from the first critical curve, into the region of high couplings and long crystals, a new critical curve is approached, where the steady-state waveguides loose stability. The second critical curve is also drawn in figure 3, and the insets to the curve show typical unstable beam profiles. The shape of these curves suggests an inverse power law dependence, and the theory confirming such a dependence is presented elsewhere [13]. At and beyond the second critical curve, dynamical solutions emerge, some examples of which have already been presented in figures 1 and 2. The time dependence varies from periodic, such as the one in figure 2, to aperiodic, such as the one in figure 1. A richer dynamical behaviour is observed in 2D, as compared to 1D, since there one has a larger phase space at disposal, and can launch beams carrying angular momentum and/or topological defects in their structure. Some examples are presented in later sections.

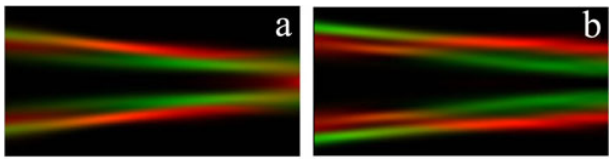

Figure 4. (a) Incoherent, $\varepsilon = 0$ and (b) coherent, $\varepsilon = 1$ interaction of two pairs of CP beams, in steady-state and the (x, z) plane. The initial offset is $4x_0$ for the in-phase beams propagating to the right and $2x_0$ for the out-of-phase beams propagating to the left. Parameters and layout as in figure 1.

3.3. Coherent and incoherent interaction

Having observed different steady-state incoherent self-trapped structures, we examine the difference between coherent and incoherent interaction of beams. It should be stressed that in this paper we are using an isotropic, local description of saturable PR media. The anisotropic, nonlocal description offers different results. In fact, in the anisotropic description the influence of the modulated component of the space charge field is reduced, and the coherent case appears similar to the incoherent case. As will be seen in a moment, the difference is not that pronounced in the isotropic approximation either.

Two steady-state solutions with the same boundary conditions but for different degrees of mutual coherence ε are shown in figure 4. CP beam components made of two pairs of beams are launched with a lateral offset. The beams to the right are in-phase, and aim at the centre of the opposite crystal face. The beams to the left are out-of-phase, and launched in parallel. Figure 4(a) displays the incoherent interaction, $\varepsilon = 0$. The beams attract, focus and overlap tightly, but the ones to the right are still capable of building an intense spot in between the other two. However, in the coherent case $\varepsilon = 1$, shown in figure 4(b), the beams focus and overlap less, and the ones to the right are expelled from the region in between the other two. Also, the timescale of the build-up dynamics is shorter for the coherent beams than for the incoherent beams.

3.4. Dynamical symmetry breaking

Of special interest are those self-trapped structures that dynamically do not converge to a steady state. Such structures represent novel time-dependent, as well as z-dependent, waveguides that cannot be described by the usual steady-state theory of spatial solitons. Whereas the z-dependence can be ascribed to the general definition of longitudinal waveguide modes, the time-dependence is a novel feature, caused by the slow response of PR crystals. In addition to the presented incoherent and symmetric cases, another example is depicted in figure 5, where a collision of the three against two power-matched coherent beams is presented, which ends in a dynamic symmetry-breaking transition to a spatiotemporal chaotic state. The initial configuration is such that the three

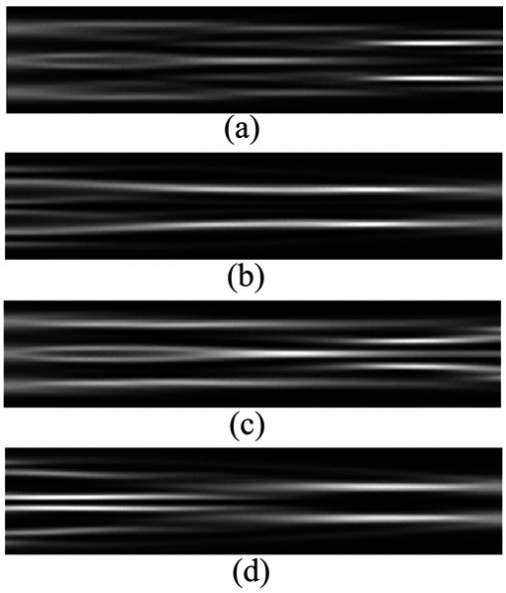

Figure 5. Symmetric unstable quasi-periodic self-organized beam structure at different times, (x, z) cross section. (a) and (c) three in-phase beams propagating to the right, (b) and (d) two out-of-phase beams propagating to the left; (a) and (b) are at $t = 40\tau_0$, (c) and (d) at $t = 90\tau_0$. The components have equal powers, $\Gamma = 10$, $\varepsilon = 1$. Other parameters as in figure 1.

beams propagating to the right interfere constructively (a)–(c), to overlap with the two counterpropagating out-of-phase beams (b)–(d). These two beams, propagating to the left, repel and overlap with the two outside-lying opposite beams. During the time evolution of this dynamical state we observe several alternations of transversely symmetrical structures, similar to the ones shown in figure 5, and identified such behaviour as a quasi-periodic self-oscillation, clearly seen in figure 6 for $t < 116\tau_0$. At that point the development of transverse symmetry-breaking instability is observed, which results in irregular spatiotemporal dynamics, shown in figure 6 for $t > 116\tau_0$.

4. Two-dimensional results

4.1. Dipole-mode vector soliton

In (2+1) spatial dimensions we reconsider some of the (1+1)D interesting cases, and then present some cases which have no 1D analogues. A general conclusion is that 2D configurations, similar to the 1D results, tend to form stable states for weaker couplings and shorter propagation distances. For stronger couplings and/or longer propagation distances, modulational instabilities set in, leading to periodic, quasiperiodic or chaotic states. We present here only the stable or rotating states that cannot be accessed by the usual steady-state theory of spatial solitons. We also confine our attention to incoherent CP beams. The parameters for the 2D numerical runs are the same for all the cases, and are: the coupling strength $\Gamma = 19.1$, the propagation distance $L = L_D/3$, the beam width $x_0 = 10\ \mu$m. For these parameters one observes only the steady-state configurations or the stable rotating ones.

Figure 7 presents the formation of a stable dipole-mode vector soliton in 2D. Our simulations indicate that if the CP components have equal powers the vector solitons formed are unstable even for relatively short thicknesses of the medium ($L \sim L_D$). The instability breaks the symmetry in the transverse plane, so that initially overlapping CP beams do not overlap after some time. In figure 7 the propagation distance is short enough for the formation of a stable displaced CP dipole-mode soliton. The incident profiles on the front and back faces of the crystal are the numerically calculated solitary solutions for the copropagating dipole-mode vector soliton.

4.2. Rotating dipoles

When a fundamental beam is counterpropagated against a vortex beam, there is no deviation of the beams during propagation through the crystal (figure 8). In time, and away from the $z = L$ face, the vortex breaks into a dipole beam that continually rotates clockwise or counterclockwise, depending on the sign of the vortex topological charge. The fundamental beam splits into a two-peaked beam that in each z-section of the transverse plane (away from the crystal faces) corotates and overlaps with the dipole beam coming from the vortex. The temporal dynamics is shown in figure 8. At $t = 5\tau_0$ the vortex has not yet broken into a dipole, and the fundamental is not yet deformed. At $t = 10\tau_0$ however, the vortex beam incident upon the back face of the crystal leaves the crystal as a dipole. This brings about the deformation of the fundamental beam, which eventually splits into two beams. Note that the dipole and the fundamental beam are shown at two different faces of the crystal, $z = 0$ and $z = L$, respectively. Watching the temporal changes, the dipole and the fundamental beam form a stable corotating dynamical state of the system (actually, the beams are counter-rotating in their propagation senses).

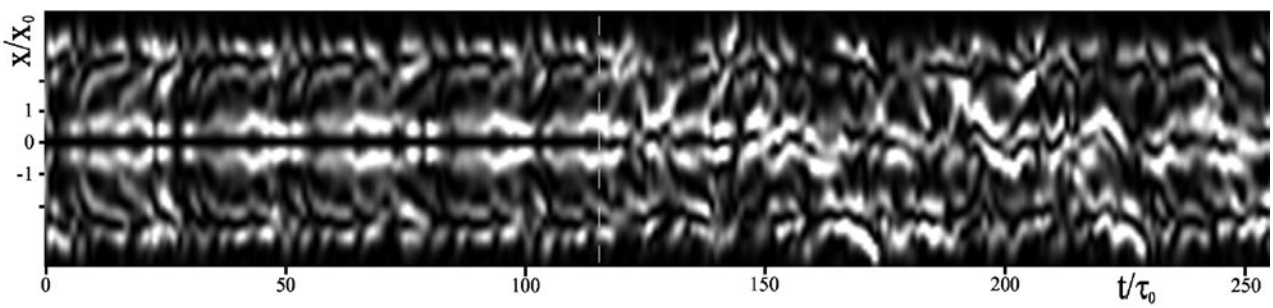

Figure 6. Temporal evolution of the output intensity distribution of the two-lobe left-propagating beam at the left face of the crystal. The dashed line at $t = 116\tau_0$ shows the place of symmetry breaking of figure 5, where the modulational instability breaks the transverse symmetry.

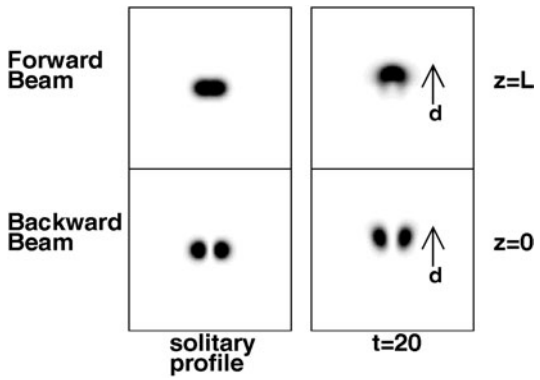

Figure 7. Counterpropagating fundamental and dipole beam. Left column, the incident profiles on the front and back faces of the crystal. Right column, the exiting profiles on the back and front faces of the crystal, after $t = 20\tau_0$. After that time the beam profiles no longer change. Vectors d point the direction in which the beams deviate during propagation.

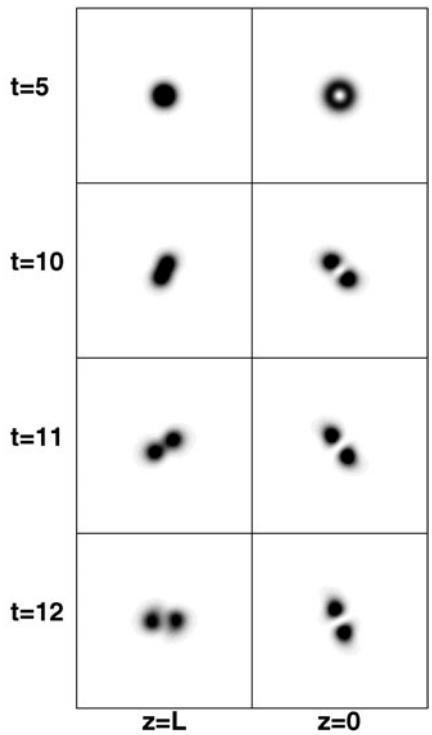

Figure 8. Temporal evolution of a fundamental beam and a CP vortex at the back and front crystal face. Left column, the fundamental beam, right column, the vortex, at different times, expressed in units of τ_0.

4.3. Colliding vortices

In the case of colliding vortices with opposite topological charges the beams also break up, but generally into more than two fragments. In figure 9 the case of two counterpropagating counter-rotating vortices is displayed, which break into three beamlets with phase shifts of $2\pi/3$. After a while the beams form stable rotating structures that do not change in time. When viewed in their exit faces, the beams form true rotating propellers [14]. Such stable rotating states, the colliding vortices and the rotating dipoles, are truly interesting for developing transverse modulational instabilities over a fraction

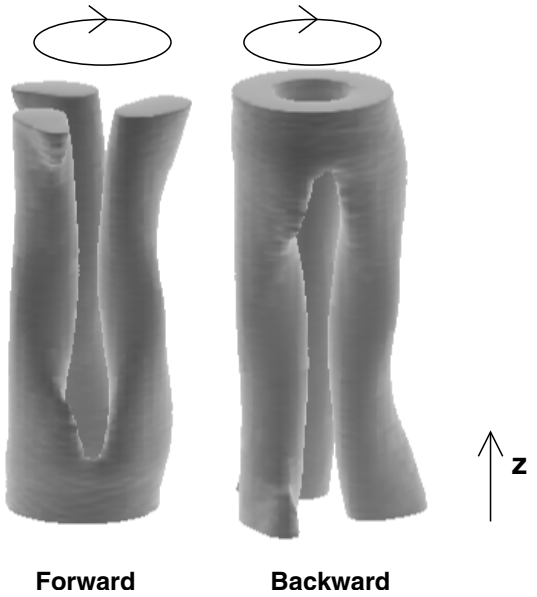

Figure 9. Iso-surface plots of two CP vortices, with charges ± 1. Upon collision the vortices break into three beamlets, which corotate continually in the sense indicated by the loops.

of diffraction length, even though they are generated in an isotropic model. Previously observed isotropic vortex vector solitons, with copropagating components, tended to propagate for tens of diffraction lengths before developing modulational instabilities.

5. Conclusions

In summary, we have developed a theory of dynamical self-trapped bidirectional optical beam structures. In counterpropagating geometry, the inclusion of time-dependent effects was found to be crucial for the formation of joint waveguiding structures. We demonstrated the generation of counterpropagating (1 + 1)D and (2 + 1)D vector solitons numerically and proposed more general classes of non-solitonic steady-state and rotating structures. A symmetry breaking transition of CP solitons into bidirectional waveguides is found, and a critical curve in the parameter plane determined. A second critical curve is discovered, separating stable waveguides from the unstable ones. The level of temporal coherence of interacting beams influences the mutual coupling due to the formation of a refractive index grating. In addition to the generation of steady-state induced waveguides, the dynamic alternation of states followed by a transverse modulational instability, as well as the onset of longitudinal modulational instabilities leading to spatiotemporal chaos were observed.

Acknowledgments

MB, AD, and AS gratefully acknowledge financial support from the Alexander von Humboldt Foundation, and for the stay and work at WWU Münster. Part of this work was supported by the Deutsche Forschungsgemeinschaft. Work at the Institute of Physics is supported by the Ministry of Science, Development and Technologies of the Republic of Serbia, under grants OI 1475 and 1478.

References

[1] Segev M (ed) 2002 *Opt. Photon. News* **13** (2) (Special issue on solitons)

[2] Haelterman M, Sheppard A P and Snyder A W 1993 *Opt. Commun.* **103** 145

[3] Cohen O *et al* 2002 *Phys. Rev. Lett.* **89** 133901
Cohen O *et al* 2002 *Opt. Lett.* **27** 2013

[4] Honda T 1993 *Opt. Lett.* **18** 598
Honda T 1995 *Opt. Lett.* **20** 851

[5] Saffman M, Zozulya A A and Anderson D Z 1994 *J. Opt. Soc. Am.* B **11** 1409

[6] Belić M, Leonardy J, Timotijević D and Kaiser F 1995 *J. Opt. Soc. Am.* B **12** 1602

[7] Arecchi F T, Boccaletti S and Ramazza P L 1999 *Phys. Rep.* **318** 1

[8] Belić M, Jander Ph, Strinć A, Desyatnikov A and Denz C 2003 *Phys. Rev.* E **68** 025601 (Rapid Communication)

[9] Weilnau C, Ahles M, Petter J, Träger D, Schröder J and Denz C 2002 *Ann. Phys., Lpz.* **9** 1

[10] Solymar L, Webb D J and Grunett-Jepsen A 1996 *The Physics and Applications of Photorefractive Materials* (Oxford: Clarendon)

[11] Sandfuchs O, Kaiser F and Belić M R 2001 *Phys. Rev.* A **64** 063809

[12] Ostrovskaya E A, Kivshar Yu S, Skryabin D V and Firth W J 1999 *Phys. Rev. Lett.* **83** 296

[13] Motzek K, Jander Ph, Desyatnikov A, Belić M, Denz C and Kaiser F 2003 *Phys. Rev.* E **68** 066611

[14] Carmon T, Uzdin R, Pigier C, Musslimani Z H, Segev M and Nepomnyashchi A 2001 *Phys. Rev. Lett.* **87** 143901